AD-A114 045 EG AND G INC SALEM MA ELECTRONIC COMPONENTS DIV F/G 9/1
NANOSECOND PULSER THYRATRONS.(U)
JAN 82 S FRIEDMAN DAAK20-80-C-0282
UNCLASSIFIED DELET-TR-80-0282-1 NL

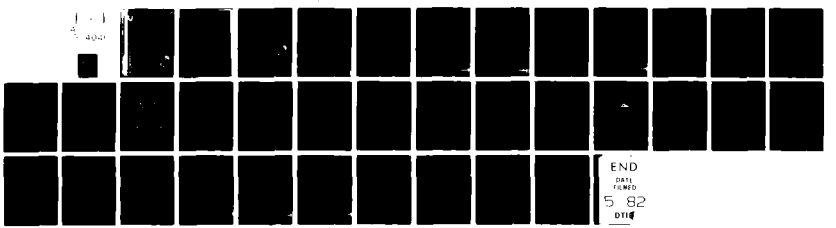

END
DATE FILMED
5 82
DTIC

Research and Development Technical Report
DELET-TR-80-0282-1

NANOSECOND PULSER THYRATRONS

Steven Friedman

EG&G, INC.
35 Congress Street
Salem, MA 01970

January 1982

First Interim Report for Period 10 July 1980 — 10 December 1980

Prepared for:
Electronics Technology & Devices Laboratory

ERADCOM

U.S. ARMY ELECTRONICS R&D COMMAND, FORT MONMOUTH, NEW JERSEY 07703

NOTICES

Disclaimers

The citation of trade names and names of manufacturers in this report is not to be construed as official Government endorsement or approval of commercial products or services referenced herein.

Disposition

Destroy this report when it is no longer needed. Do not return it to the orginator.

UNCLASSIFIED

SECURITY CLASSIFICATION OF THIS PAGE (When Data Entered)

REPORT DOCUMENTATION PAGE		READ INSTRUCTIONS BEFORE COMPLETING FORM
1. REPORT NUMBER DELET-TR-80-0282-1	2. GOVT ACCESSION NO. AD-A114 045	3. RECIPIENT'S CATALOG NUMBER
4. TITLE (and Subtitle) Nanosecond Pulser Thyratrons		5. TYPE OF REPORT & PERIOD COVERED First Interim 10 July 1980 – 10 Dec 1980
		6. PERFORMING ORG. REPORT NUMBER
7. AUTHOR(s) Steven Friedman		8. CONTRACT OR GRANT NUMBER(s) DAAK20-80-C-0282
9. PERFORMING ORGANIZATION NAME AND ADDRESS EG&G, Inc. 35 Congress Street Salem, MA 01970		10. PROGRAM ELEMENT, PROJECT, TASK AREA & WORK UNIT NUMBERS 62705 1L162705 AH94.01.03
11. CONTROLLING OFFICE NAME AND ADDRESS Electronics Technology and Devices Lab (ERADCOM) ATTN: DELET-BG Fort Monmouth, NJ 07703		12. REPORT DATE January 1982
		13. NUMBER OF PAGES 33
14. MONITORING AGENCY NAME & ADDRESS (if different from Controlling Office)		15. SECURITY CLASS. (of this report) Unclassified
		15a. DECLASSIFICATION/DOWNGRADING SCHEDULE

16. DISTRIBUTION STATEMENT (of this Report)

Approved for public release; distribution unlimited.

17. DISTRIBUTION STATEMENT (of the abstract entered in Block 20, if different from Report)

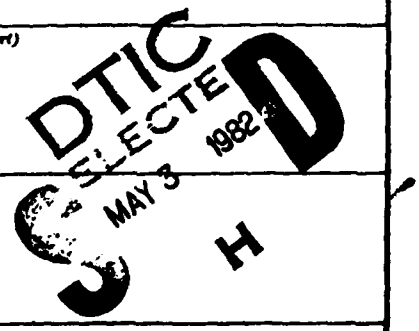

18. SUPPLEMENTARY NOTES

19. KEY WORDS (Continue on reverse side if necessary and identify by block number)

Pulser
Nanosecond
Thyratron Circuit
Pulse Sharpener
Capacitor

20. ABSTRACT (Continue on reverse side if necessary and identify by block number)

We have constructed a thyratron is constructed capable of meeting the Type II requirements for voltage, peak current and average power, and have characterized its resistive fall time, recovery time, and forward voltage holdoff as functions of pressure and triggering configuration. A low inductance circuit has been built, incorporating the thyratron, a 5 nF fast discharge capacitor, and a 60 pF capacitor to simulate the loading effect of a magnetron or EIO. A theoretical model for the circuit which includes the effects of thyratron resistance (time varying), and inductance

(continued)

cont

DD FORM 1 JAN 73 1473 EDITION OF 1 NOV 65 IS OBSOLETE

UNCLASSIFIED

SECURITY CLASSIFICATION OF THIS PAGE (When Data Entered)

20. Abstract (continued)

cont → ~~has been~~ was developed. The resistive fall time decreases with rising pressure, but more slowly than predicted by gas breakdown theory, suggesting that it is being limited by the internal design of the thyratron. Fall times of only around 3 ns are obtainable before the pressure gets too high, (0.9 torr), for the 50 μs recovery time required for 20 kHz operation. This will necessitate experimentation with ferrites to delay the current rise until the anode fall is over. Electrode design modifications to decrease the fall and recovery times will also be tested. The 6 kv forward holdoff required under Type II conditions has been attained at pressures up to 1.3 torr by use of a fast pulse charging.

ABBREVIATIONS AND SYMBOLS

C	Load capacitance
C_0	Storage capacitor capacitance
E_r	Thyratron reservoir voltage
EIO	Extended interaction oscillator
i	Current (instantaneous)
kv	Kilovolts (pulsed)
kV	Kilovolts (DC)
L	Total circuit inductance (including thyratron)
L_C	Total circuit inductance minus thyratron inductance
L_0	Inductance of storage capacitor
L_T	Thyratron inductance
nF	Nanofarads
nH	Nanohenries
ns	Nanoseconds
p	Gas pressure
pF	Picofarads
ps	Picoseconds
q	Charge on load capacitor
q_0	Charge on storage capacitor
R	Thyratron resistance
t	Time
t_f	Thyratron resistive fall time
t_r	Thyratron recovery time
V	Load voltage
V_0	Initial storage capacitor voltage
Z_0	Transmission line impedance
μs	Microseconds
τ	e-folding time of thyratron resistance

TABLE OF CONTENTS

LIST OF ILLUSTRATIONS

1 FOREWORD

This First Interim Technical Report presents the results of the first six months of a program of research and development conducted under ERADCOM Contract DAAK20-80-C-0282, entitled "Nanosecond Pulser Thyratrons," and covers the period 10 July 1980 to 10 December 1980. Experimental results obtained through 30 December 1980 are also included to ensure that this report is up to date.

The work described herein was performed by EG&G, Inc., Electronic Components Division, 35 Congress Street, Salem, Massachusetts 01970.

2 INTRODUCTION AND SUMMARY

a. Project Goals

The ultimate goal is to develop instant start thyratrons and circuits capable of meeting the two sets of requirements listed below:

	Type I	Type II
Peak Forward Voltage	20 kV	6 kV
Peak Anode Current	400 amps	360 amps
Pulse Rise Time (10-90%)	3.0 ns	1.0 ns
Load Capacitance (50% stray capacitance)	60 pF	60 pF
Burst Time	5-30 min	5-30 min
Off Time	120 min	120 min
Pulse Repetition Rate	20 kHz	20 kHz
Maximum Duty Cycle	6×10^{-4}	2×10^{-4}
Life	1000 cycles	1000 cycles
Jitter	100 ps	100 ps

These requirements immediately pose two difficulties. First, the extremely short current rise times require thyratron operation at high internal pressures inimical to the fast recovery needed for 20 kHz operation. Second, the short current rise times demand very low circuit inductance, requiring close integration of thyratron, storage capacitor, and load.

The goals for the first stage of this project were:

1) To construct low inductance thyratrons capable of meeting the current, voltage, and average power requirements, and to measure their switching times, recovery times, and voltage holdoff.

2) To construct and test low inductance circuits with simulated loads, first without ferrites to find the limits of "unassisted" thyratron operation, and then, if necessary, with ferrites to decrease the current rise time by delaying it until after the resistive fall.(1)

3) To theoretically analyze the test results to determine quantitatively how the current rise time is affected by thyratron inductance and resistive fall time.

Progress made during the first six months of the project is summarized briefly in the remainder of this section, and in detail below.

b. Thyratron Construction and Characterization

The Type II conditions were considered first because the lower voltage and average power requirements allowed smaller, cheaper, and more easily constructed thyratrons and circuit assemblies. The thyratron chosen was an HY-3013; basically an HY-1802 shortened for lower inductance, with an auxiliary grid added so that keep-alive could be employed to increase the current rise rate. The inductance was further reduced by use of annular control grid slots and an annular anode stud (Figure 1). This version of the tube was designated HY-3013L s/n 001. When surrounded by a close-fitting current return, the tube had a theoretical inductance of about 8 nH. The reservoir was filled to twice the normal amount to allow operation at relatively high pressures without overheating the filaments. The reservoir calibration is shown in Figure 2.

The resistive fall time, recovery time, and voltage holdoff were measured as functions of pressure and triggering configuration (magnitude and location of the trigger pulse, DC reverse grid bias, and keep-alive). The most important result is that while record anode fall times were achieved (2 ns), these are not fast enough for 1 ns current rise times, and require too high a pressure for 20 kHz operation (due to recovery failure). Therefore, ferrites will probably be required to delay the current rise until after the resistive fall is completed.

c. Low Inductance Circuit and Simulated Load

The load was simulated by a pure 60 pF capacitance, so that the basic circuit was as diagrammed in Figure 3. R is the time-dependent thyratron resistance, L the total circuit inductance (including the thyratron), and C_0 the fast-discharge storage capacitor (initially pulse-charged to V_0 = 6 kv). The objective under Type II conditions is to charge the 60 pF capacitor, C, to voltage V_0 = 6 kv in 1 ns or less. If thyratron resistance is neglected,

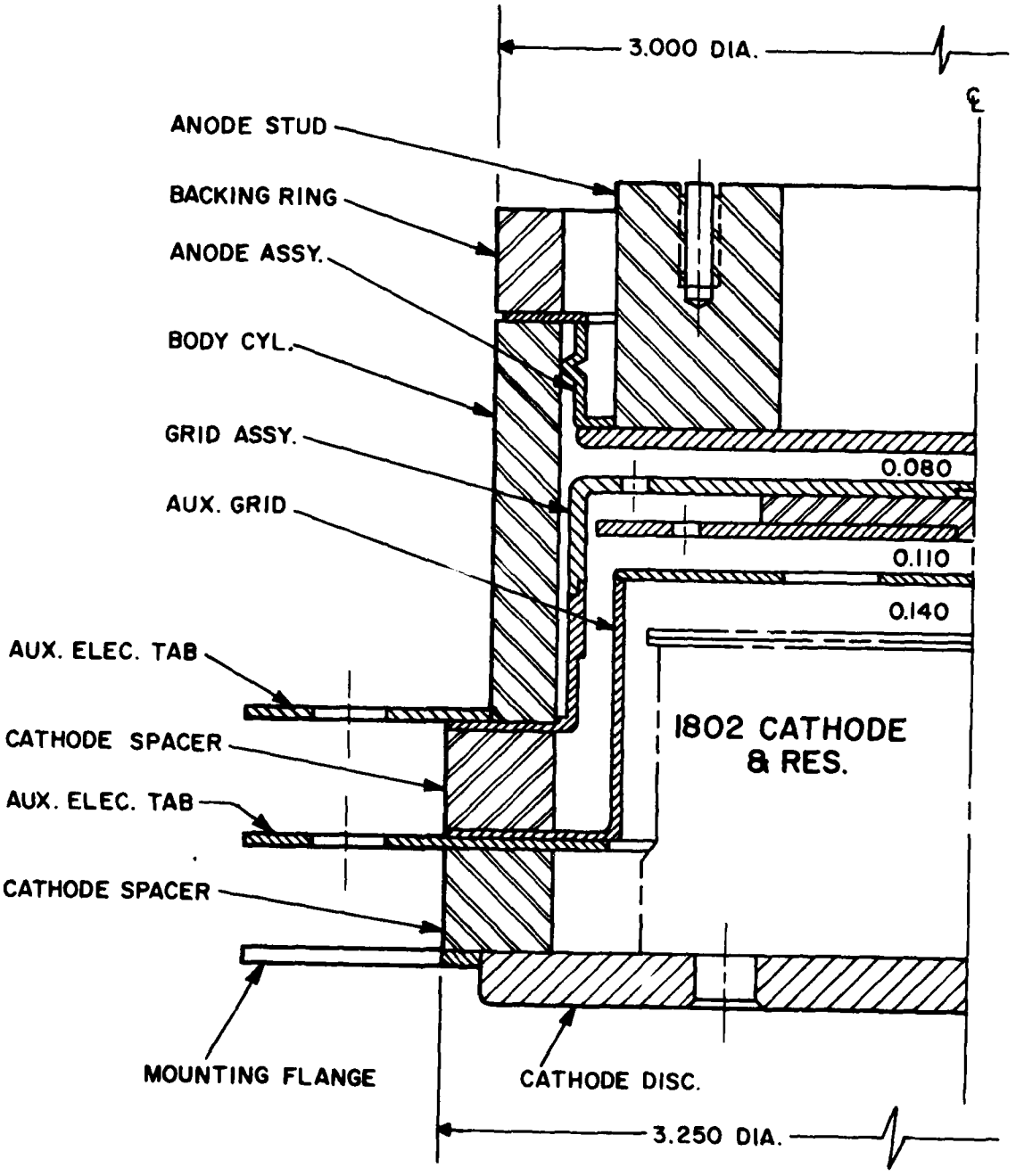

Figure 1. HY-3013L s/n 001 low inductance thyratron.

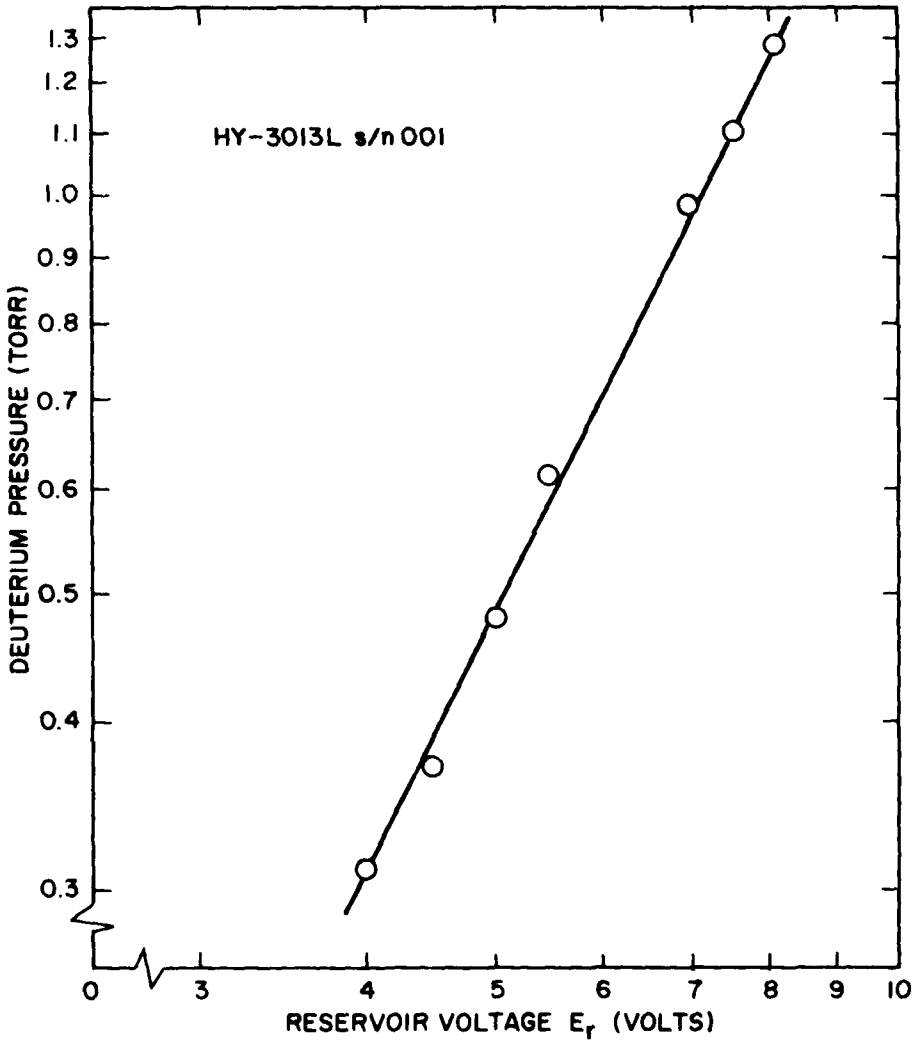

Figure 2. HY-3013L s/n 001 reservoir calibration.

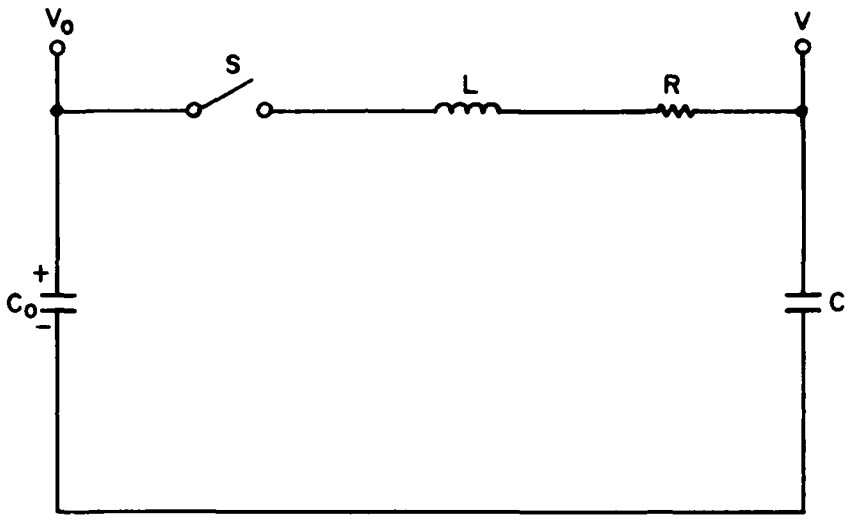

Figure 3. Basic thyratron and load circuit. (S is a perfect switch. Thyratron inductance is included in L. R is the thyratron resistance, which is time dependent. V_0 is the voltage across C_0 before switch S closes. C is the capacitive load.)

then the voltage V across C is given by $V = V_0 (1-\cos(t/\sqrt{LC}))$, assuming $C \ll C_0$. Therefore, L must be $\lesssim$ 7 nH. Allowing C to charge from 10% of V_0 to 90% of V_0 in 1 ns relaxes this requirement to $L \lesssim 17$ nH. This low value of inductance was achieved as shown in Figure 4a. The ground return is coaxial and has an inside diameter only 0.100 inch larger than the thyratron and storage capacitor. The 60 pF load is an integral part of the structure; no leads are used. To protect against flashover, the entire assembly is immersed in oil. Figure 4b shows the equivalent circuit plus the pulse charging circuit; pulse charging allows 6 kv holdoff to be maintained at pressures up to 1.3 torr. The only diagnostic is a fast high voltage probe of the type developed by Sarjeant and Alcock[2] used in conjunction with a Tektronix 7834 oscilloscope and 7A19 50-ohm plug-in to give an overall diagnostics rise time of 0.9 ns, verified using a 250 ps rise time pulse generator. The probe also serves to discharge the 60 pF load between pulses; its resistance is 3.3 kilohms.

The assembly successfully holds off 6 kv, and the load appears to be charging in a time comparable to the thyratron resistive fall time. Only low repetition rate operation (around 1 Hz) has been attempted.

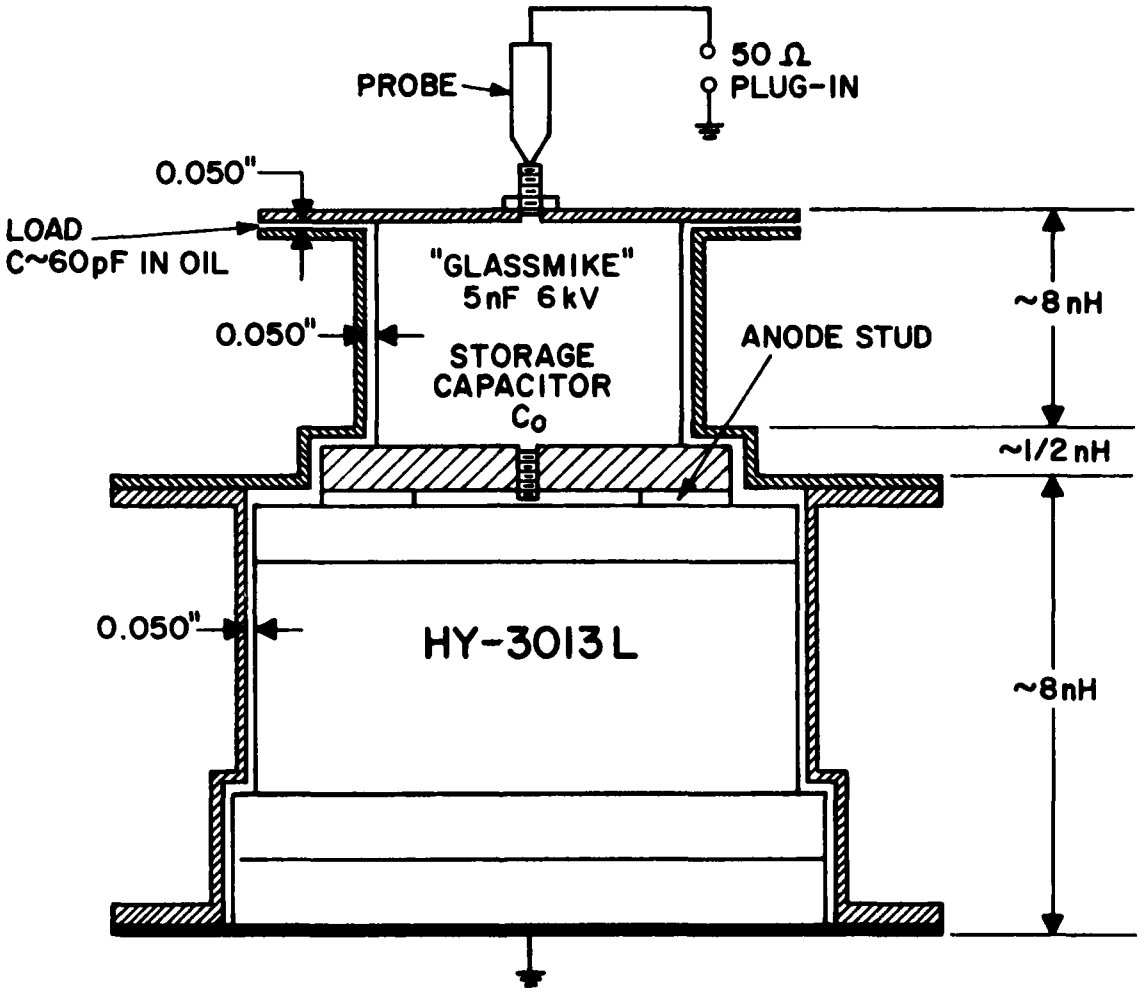

Figure 4a. Low inductance circuit assembly. (Cross-hatched pieces are aluminum. Entire assembly is immersed in oil to avoid flashover. The 5 nF capacitor is charged by a 6 kv pulse applied at the anode stud end.)

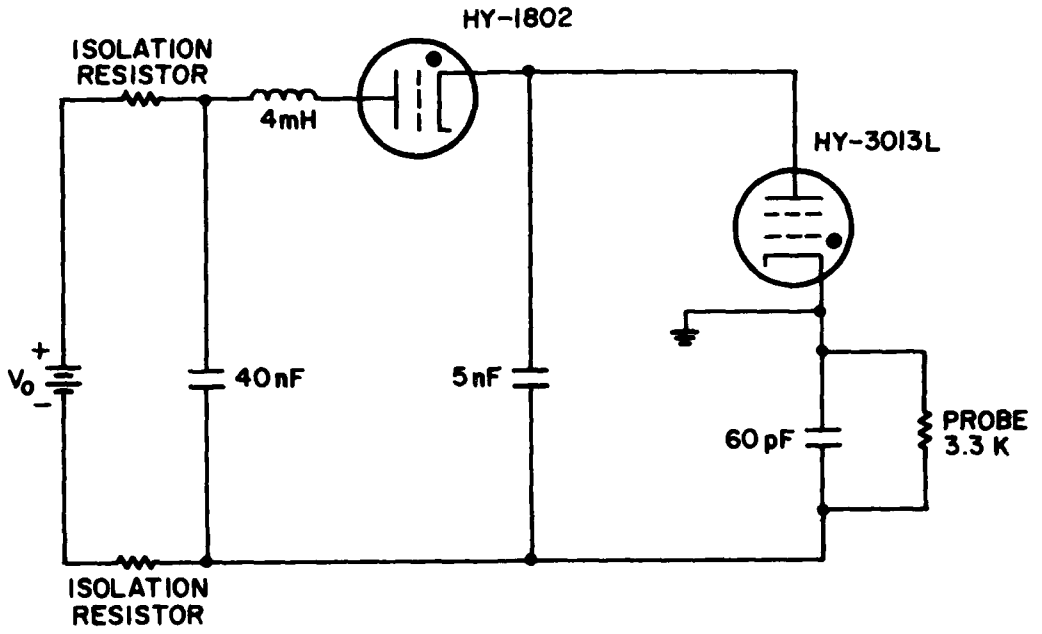

Figure 4b. Equivalent low inductance circuit and pulse charging circuit. (The 40 nF capacitor is charged to 3 kv, which resonantly doubles to 6 kv across the 5 nF capacitor when HY-1802 is triggered. The probe capacitance is much less than 60 pF.)

3 THYRATRON CHARACTERIZATION

a. Resistive Fall Time

Without ferrites to delay the current rise, the thyratron current rise time cannot be shorter than resistive fall time t_f; hence, the importance of knowing the latter. The circuit and diagnostics used for the measurement are shown in Figure 5. The inductive component of the anode fall was eliminated by making circuit inductance L_C much larger than thyratron inductance L_T, so that $L_T \cdot di/dt << V_0$.

The variable to which t_f is most sensitive is pressure, p; basic gas breakdown theory predicts $t_f \propto 1/p^2$.(3) The measured dependence of t_f on p is shown in Figure 6, along with the theoretical curve $t_f = const/p^2$, normalized to the lowest pressure data point. Clearly, t_f is being limited by factors other than basic gas breakdown, suggesting that changes in internal electrode design could speed the fall time. In particular, larger and/or more numerous grid apertures, and smaller inter-electrode spacings, are being considered. However, these could have the trade-off effect of reducing voltage holdoff.

The triggering techniques used in an attempt to decrease t_f were: use of high trigger voltage (up to 2.5 kv, as compared to the 300 volts actually required for commutation); keep-alive; and reverse control grid bias to delay commutation until the trigger plasma reached maximum density.(4) These techniques had been found to increase the current rise rate in past experiments(4,5), but were found here to have no effect on t_f.

b. Recovery Time

A 20 kHz repetition rate requires a thyratron recovery time, t_r, of 50 ns or less. Figure 7 plots the experimental values of t_r vs pressure, along with a plot of resistive fall time, t_f, reproduced from Figure 6. It can be seen that the pressure required to achieve resistive fall times approaching 1 ns is incompatible with 20 kHz operation for the thyratron as presently constructed.

Experiments with larger tubes have shown that recovery time can be reduced by nearly an order of magnitude by employing additional baffles to increase the electrode surface area and hence the plasma loss rate. Reductions in the inter-electrode spacings should also yield a faster plasma loss rate, and hence faster recovery.

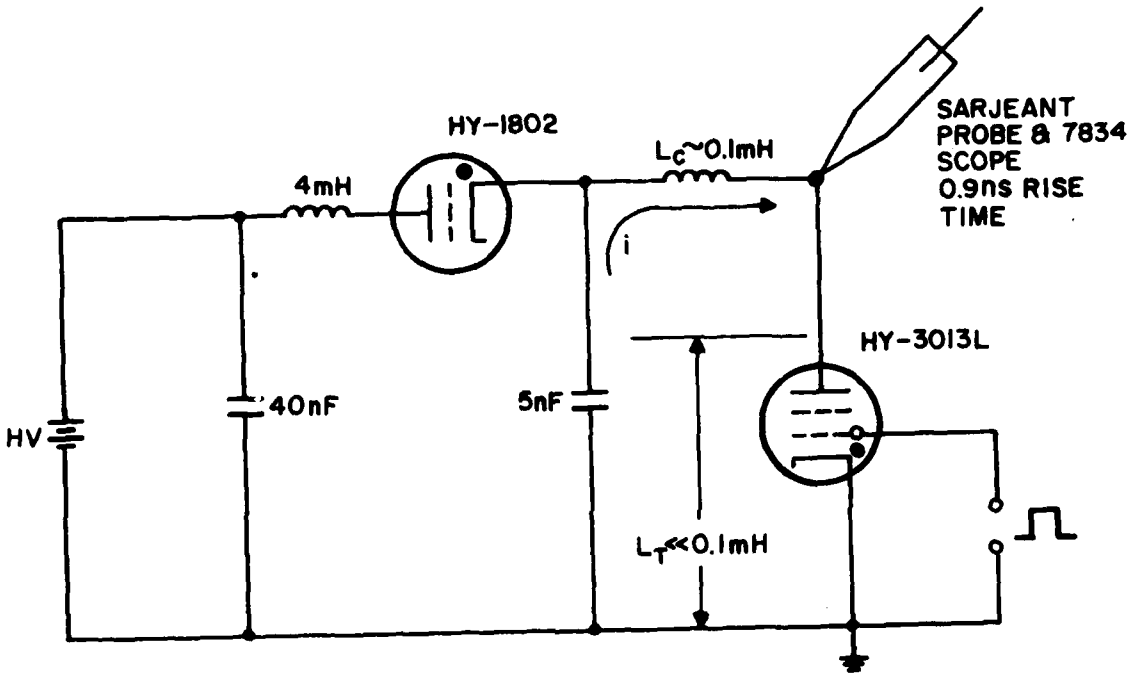

Figure 5. Circuit for measuring resistive fall time.

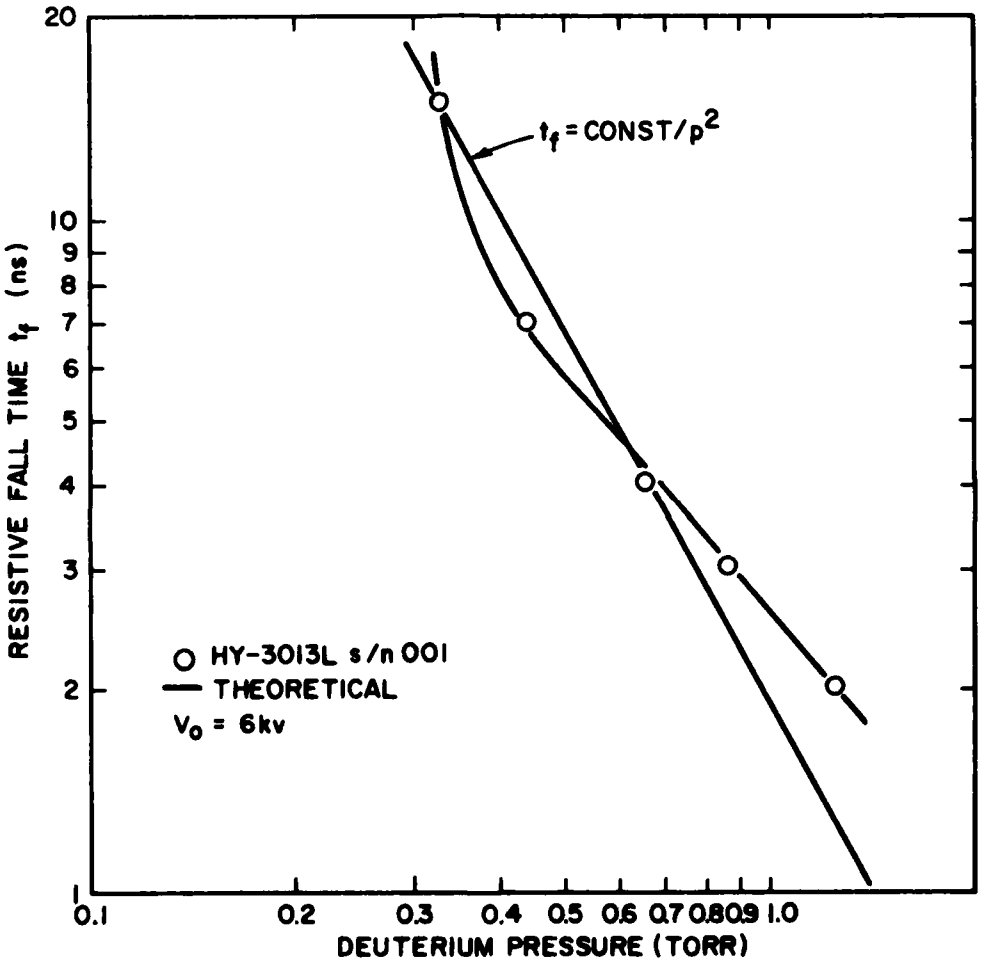

Figure 6. Resistive fall time vs pressure. The theoretical curve is normalized to intersect the experimental curve at the lowest pressure data point. Lower values of t_f could not be obtained because the thyratron failed to hold off 6 kv for pressures above 1.25 torr.

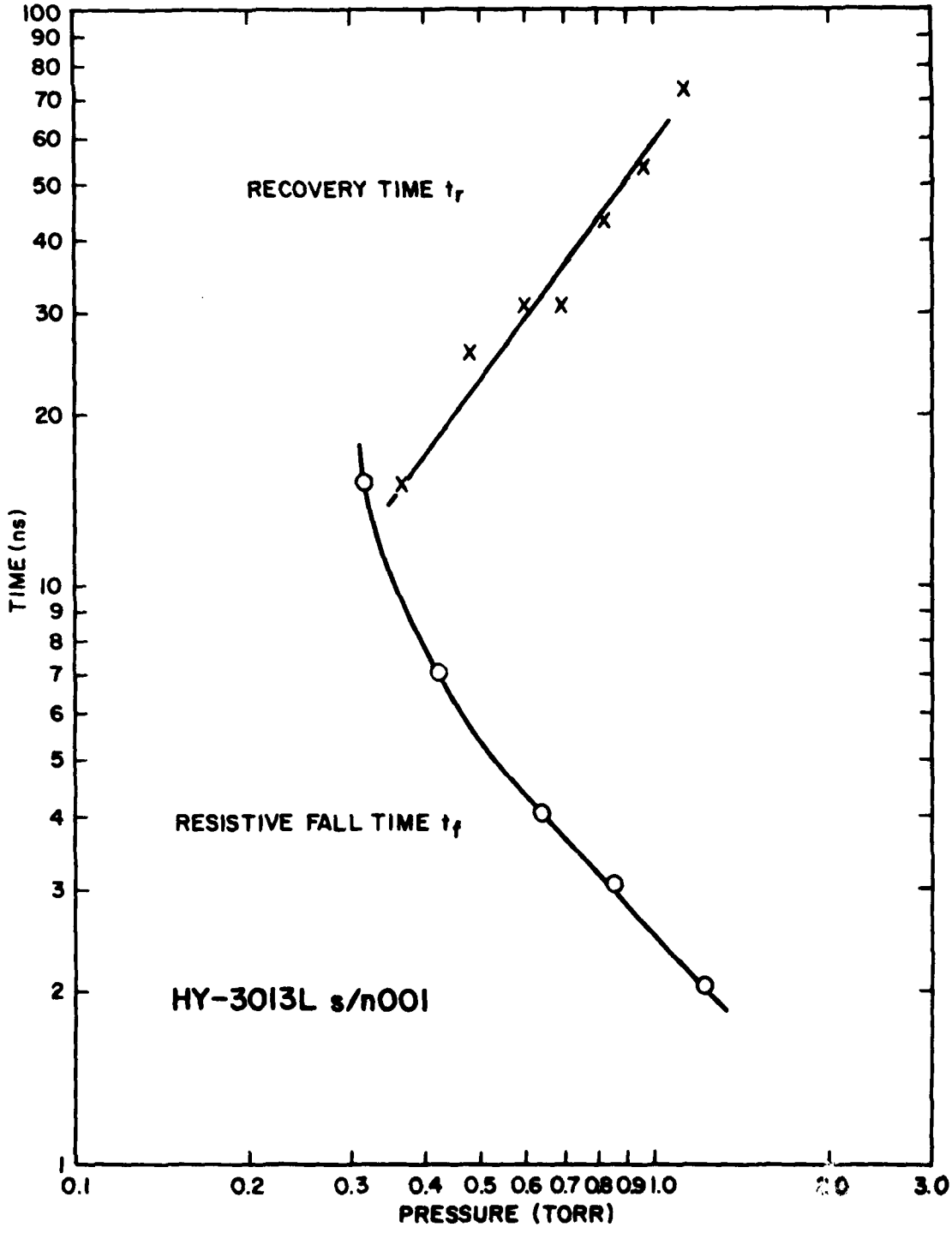

Figure 7. Recovery time vs pressure.

To avoid the power dissipation problems associated with 20 kHz operation, the recovery time measurements were made by firing the thyratron in 2-pulse bursts with, for example, 50 μs between pulses and 1 second between bursts. Since trigger modules capable of producing two such closely spaced pulses of sufficient amplitude to commutate the HY-1802 and HY-3013L thyratrons were unavailable, the multiple trigger module circuit shown in Figure 8a was used. First, trigger module T1 fired, triggering the HY-1802 and also sending a signal to pulse generator P1. After an adjustable delay of a few μs, by which time C_0 had charged to 6 kv, P1 sent a pulse to T2, causing it to trigger HY-3013L and thus discharge C_0 through HY-3013L via a 12-ohm resistor, which limited the current to a value comparable to that required under Type II conditions (6 kv x 60 pF/1 ns = 360 amps). P1 simultaneously sent a pulse to P2, which, after an adjustable delay, triggered T3. This again fired the HY-1802, charging C_0 a second time. If HY-3013L had recovered, this second charging pulse would have reached 6 kv and then drained off through the 10 k resistor. If not, HY-3013L lost holdoff and discharged C_0 before 6 kv was reached, as shown in the oscillogram of Figure 8b.

Reverse biasing of the control and auxiliary grids was tried, but failed to affect the recovery time.

c. Forward Voltage Holdoff

To determine how long 6 kv could be held off at various pressures, the charging voltage rise time was reduced to 2.5 μs (by eliminating the 5 nF capacitor, leaving only the 150 pF capacitance of the HY-3013L itself to be charged), and the Sarjeant probe was replaced by a 100-megohm TEK probe to prevent the charging voltage from decaying significantly during the holdoff time. The tube held off 6 kv DC for reservoir voltages $E_r < 6.0$ V. From 6-8 V, the tube held off for several tens of μs. At 8 V the holdoff time dropped to less than 1 μs. This drop was so precipitous that it was not possible within experimental error to meaningfully plot holdoff time vs pressure. For all practical purposes, HY-3013L s/n 001 loses 6 kv holdoff at $E_r = 8.0$ V (about 1.3 torr).

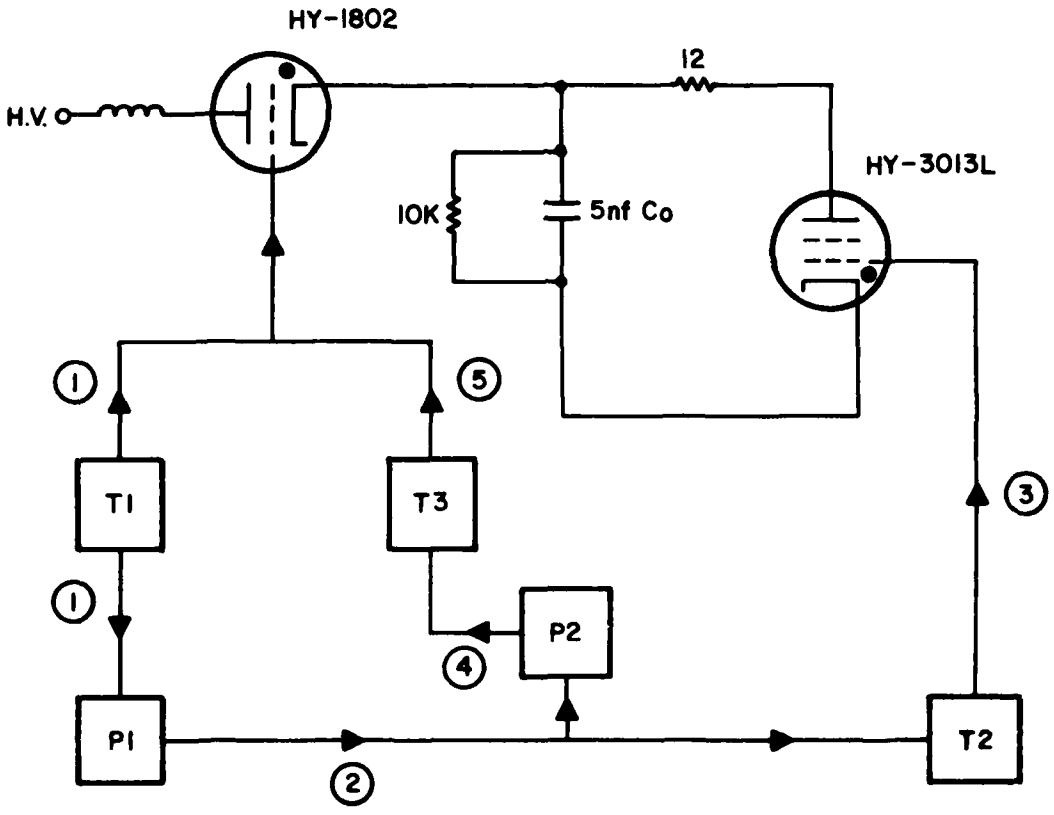

LEGEND:

(1) T1 FIRES HY-1802, CHARGING C_o AND TRIGGERING P1.
(2) P1 TRIGGERS P2 AND T2 AFTER A FEW μs DELAY.
(3) T2 FIRES HY-3013L, DUMPING C_o.
(4) AFTER TENS OF μs DELAY, P2 TRIGGERS T3.
(5) T3 FIRES HY-1802, RECHARGING C_o.

NOTE:

ABOUT 1 SECOND LATER, T1 FIRES AGAIN, RESTARTING THE CYCLE.

Figure 8a. Circuit for measuring recovery time.

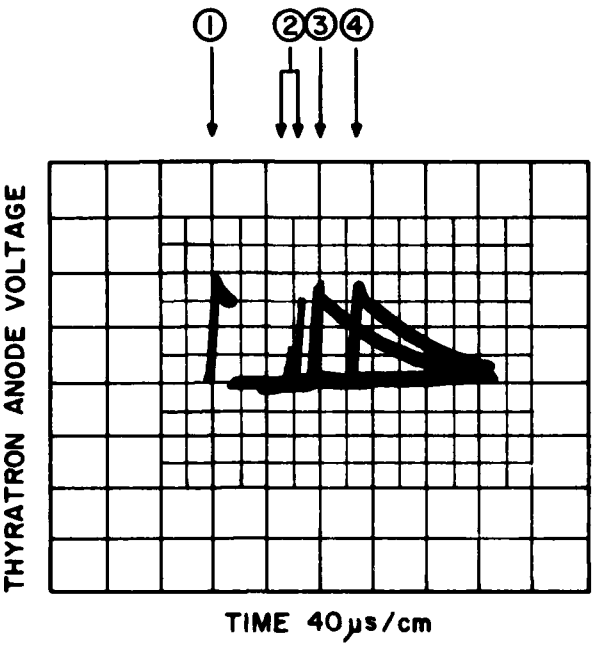

LEGEND:

① INITIAL 6kv PULSE.

② SECOND PULSES ARRIVE BEFORE THYRATRON HAS RECOVERED.

③,④ SECOND PULSES WHEN THYRATRON HAS RECOVERED.

NOTE: THE RECOVERY TIME FOR THIS CASE IS 60μs

Figure 8b. Typical recovery time data for HY-3013L s/n 001.

d. Conclusions

While modifications of the internal electrode design of HY-3013L s/n 001 may possibly enable the thyratron to simultaneously meet the Type II current rise time, repetition rate, and voltage holdoff requirements, ferrite current delay will probably be required in addition, to allow operation at lower pressures without the current rise rate being limited by the resistive fall time.

4 LOW INDUCTANCE CIRCUIT ANALYSIS

a. Inductance Calculations and Measurements

The low inductance circuit, including storage capacitor, thyratron, and 60 pF load, is shown in Figure 9. The indicated inductance value for the thyratron section is theoretical and assumes an internal current distribution uniform out to the control grid slot diameter. The true current distribution is undoubtedly more complex, given the rapid rise time, but experience has shown that current rise rates calculated on this assumption are in good agreement with the experiments.(4)

The inductance of the 5 nF fast discharge capacitor was determined by measuring its resonant frequency. The circuit designed for this purpose may prove useful in future low inductance design work, and thus is described in detail here.

Inductance L_0 of PFN capacitor C_0 and its current return was found by measuring the resonant frequency using a VHF oscillator. The circuit is shown in Figure 10. Resonance was detected by sensing at what frequency the voltage across the series combination of L_0 and C_0 went through a minimum. To ensure reliable results, the following precautions were taken:

1) The length of the circuit was kept to a small fraction of a wavelength. (At 100 MHz, the free space wavelength is 3 meters. The distance from the oscillator to C_0 was about 15 cm.)

2) Resistor R was chosen to be >> 50 ohms, and also to be >> its stray capacitive and inductive impedances. Thus, the VHF oscillator always sensed a nearly constant impedance. This helped to minimize changes in output voltage with frequency. The small variations that did occur were monitored and corrected by adjusting the oscillator amplitude control.

First, C_0 was measured using a digital capacitance meter and found to be 5.1 nF. The measured resonant frequency was 25 MHz, giving 14 nH inductance. A series of measurements using different lengths of connectors established that 6 nH of this inductance was due to the General Radio "T" connector on which C_0 was mounted, leaving $L_0 \simeq 8$ nH.

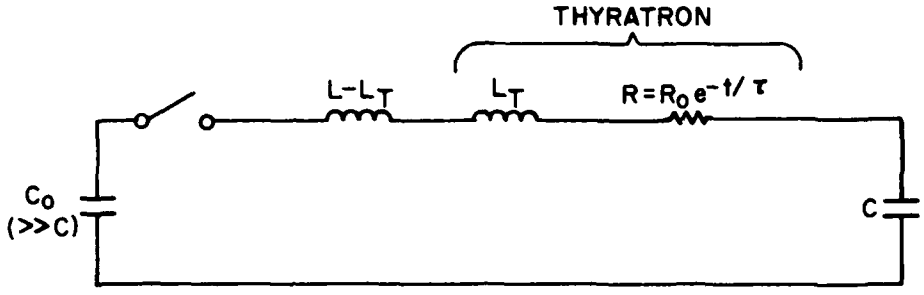

Figure 9. PFN equivalent circuit, including thyratron inductance and resistance.

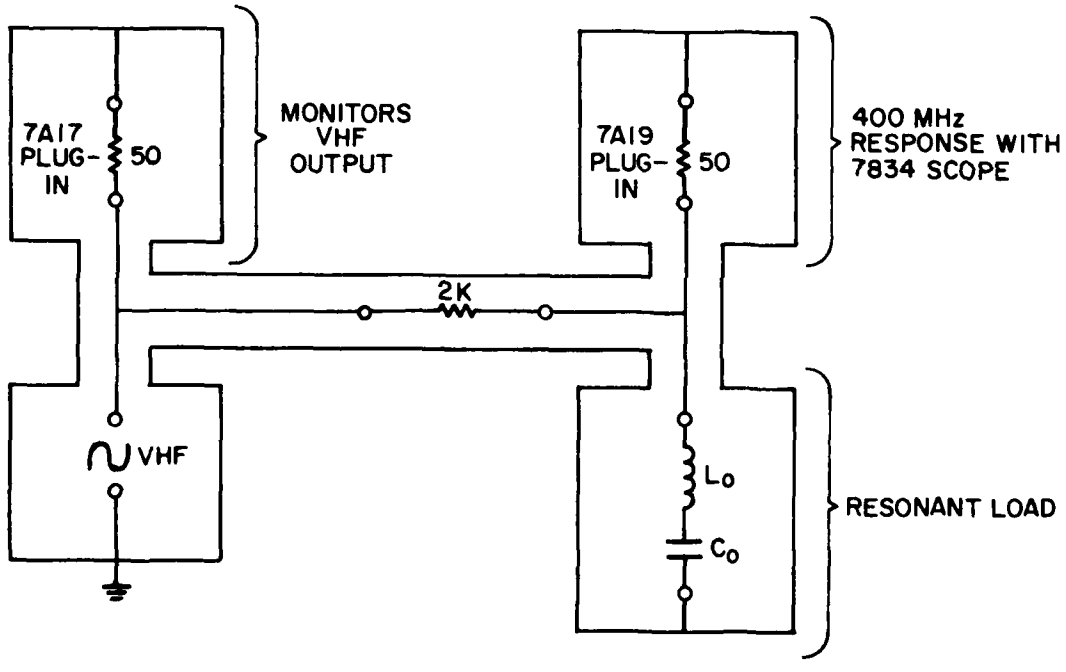

Figure 10. Circuit for measuring nanohenry inductances. General Radio and BNC type connectors used throughout.

This same procedure can be used to measure the inductance of the load, and of future circuit components.

b. Theoretical Analysis of Load Capacitor Charging Time

In the equivalent circuit of Figure 9, L and L_T are the total circuit and thyratron inductances, respectively. R is the thyratron resistance, assumed to decay exponentially with a characteristic decay time, τ, simulating the resistive fall. Initially, PFN capacitor C_0 is charged to voltage V_0 and C is uncharged. Denoting the charges on C_0 and C by q_0 and q, respectively, Kirchoff's equation is

$$\frac{q_0}{C_0} = L\frac{di}{dt} + Ri + \frac{q}{C} \tag{1}$$

From charge conservation,

$$q_0 + q = CV_0, \quad i = \dot{q} = -\dot{q}_0 \tag{2}$$

giving, assuming $C_0 >> C$,

$$V_0 = L\ddot{q} + R\dot{q} + \frac{q}{C} \tag{3}$$

Load voltage $V = q/C$. Substituting, dividing through by V_0, and defining $x \equiv V/V_0$ gives

$$\ddot{x} + \frac{R}{L}\dot{x} + \frac{x}{LC} - \frac{1}{LC} = 0 \tag{4}$$

Now substitute $R = R_0 \exp-(t/\tau)$ and define $y \equiv t/\tau$.

$$\frac{d^2x}{dy^2} + \frac{R_0\tau}{L}e^{-y}\frac{dx}{dy} + \left(\frac{\tau}{\sqrt{LC}}\right)^2 x - \left(\frac{\tau}{\sqrt{LC}}\right)^2 = 0 \tag{5}$$

Finally, for R_0 substitute K L/C, giving

$$\frac{d^2x}{dy^2} + K\frac{\tau}{\sqrt{LC}}e^{-y}\frac{dx}{dy} + \left(\frac{\tau}{\sqrt{LC}}\right)^2 x - \left(\frac{\tau}{\sqrt{LC}}\right)^2 = 0 \tag{6}$$

This equation has the general form.

$$\frac{d^2x}{dy^2} + f(y)\frac{dx}{dy} + gx - g = 0 \tag{7}$$

where

$$g = (\tau/LC)^2 \qquad f = K\sqrt{g}\, e^{-y} \tag{8}$$

In preparation for numerical solution, convert this second order differential equation into two first order equations by introducing a new variable, Z.

$$Z = dx/dy$$

$$\frac{dz}{dy} = -f\frac{dx}{dy} - gx + g \tag{9}$$

Next, divide the y axis into intervals $dy/2 \equiv \Delta$.

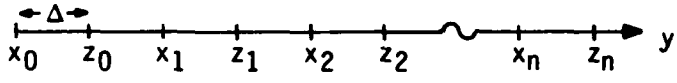

(10)

The two first order differential equations can now be written as difference equations:

$$x_n = x_{n-1} + z_{n-1}\Delta$$

$$z_n = z_{n-1} + \left(\frac{dz}{dy}\right)_{x = x_n}\Delta \tag{11}$$

resulting in, finally,

$$x_n = x_{n-1} + z_{n-1}\Delta$$

$$z_n = \frac{z_{n-1} - g(x_{n-1})}{1 + f_n\,\Delta}\,, \quad f_n = K\sqrt{g}\, e^{-n\Delta} \tag{12}$$

Equations (10), (11), and (12) are solved in turn, starting with $x_0 = 0$, $y_0 = 0$. (Since Z_0 is actually removed from $y = 0$ by distance Δ, it is not exactly zero. However, the error is negligible if Δ is sufficiently small.)

As Δ gets smaller, the solution gets more accurate but takes longer to compute. $\Delta = 0.1$ is a reasonable compromise.

For the sake of definiteness, τ will be chosen to be 1/4 the total resistive fall time.

Finally, a value must be chosen for K. Recall that $K = R_0/\sqrt{L/C}$ and that R_0 (the thyratron resistance at $t = 0$), is, in principle, infinite. The assumption of a non-infinite value for K is equivalent to beginning the solution at some time $t_1 > 0$, in which case the load voltage waveform for $0 < t < t_1$ is not generated. This is all right, however, because the load voltage rises very slowly near $t = 0$, and only begins its sharp rise later. So long as t_1 comes before this sharp rise, the 10-90% rise time will be accurately depicted. Experience has shown that $K = 1000$ is a good choice.[4] Larger values prolong the computation without revealing significant additional information.

This simple numerical method can be done in a few minutes on a programmable pocket calculator. Its usefulness and accuracy have been proven elsewhere,[4] and its appropriateness for this work will be evaluated when appropriate experimental data has been generated.

5 CONCLUSIONS AND FUTURE PLANS

The resistive fall time, recovery time, and forward voltage holdoff of HY-3013L s/n 001 are not far from the Type II requirements. Fulfilling the remaining requirements will require either modifying the internal thyratron structure, using ferrite current delay, or both.

Our plans for the immediate future are to:

1) Determine the effect of triggering configuration on the charging time of the 60 pF capacitor in the low inductance circuit. This will include varying the magnitude and location of the trigger pulse, grid bias, and keep-alive.

2) Compare low inductance circuit operation with theory.

3) Explore the use of ferrites to shorten the current rise time by delaying the current rise until the resistive fall is complete.

4) Construct and test HY-3013L type thyratrons with internal modifications designed to speed the resistive fall and to promote faster recovery.

6 REFERENCES

(1) Creedon, J., and Schneider, S., Proc. Fifth Symposium on Hydrogen Thyratrons and Modulators, Ft. Monmouth, New Jersey, May 1958, p. 145.

(2) Sarjeant, W., and Alcock, A., Rev. Sci. Instrum., 47, 10, 1976, p. 1283.

(3) Goldberg, S., and Rothstein, J., Advances in Electronics and Electron Physics, Vol. XIV, Academic Press, New York, 1961, p. 207.

(4) Caristi, R., et al., IEEE Trans. Electron Devices ED-26, 10, 1427, 1979.

(5) Friedman, S., et al., 1978 Thirteenth Pulsed Power Modulator Symposium, Buffalo, New York, June 1978, p. 129.

DISTRIBUTION LIST

101 Defense Technical Info Ctr
ATTN: DTIC-TCA
Cameron Station (Bldg 5)
012 Alexandria, VA 22314

102 Director
National Security Agency
ATTN: TDL
001 Fort George G. Meade, MD 20755

103 Code R123, Tech Library
DCA Defense Comm Engrg Ctr
1860 Wiehle Avenue
001 Reston, VA 22090

104 Defense Communications Agency
Technical Library Center
Code 205 (P.A. Tolovi)
002 Washington, DC 20305

200 Office of Naval Research
Code 427
001 Arlington, VA 22217

205 Commanding Officer
Naval Research Laboratory
ATTN: Code 2627, 1409, 5270
(In Turn)
001 Washington, DC 20375

207 Cdr, Naval Surface Weapons Ctr
White Oak Laboratory
ATTN: Library, Code WX-21
001 Silver Spring, MD 20910

209 Commander (Air-5471/5473)
Naval Air Systems Command
002 Washington, DC 20361

210 Commandant, Marine Corps
HQ, US Marine Corps
ATTN: Code LMC, INTS (In Turn)
001 Washington, DC 20380

212 Command, Control & Comm Div.
Development Center
Marine Corps Dev & Educ Cmd
001 Quantico, VA 22134

300 AUL/LSI 64-285
001 Maxwell AFB, AL 36112

301 Rome Air Development Center
ATTN: Documents Library (TSLD)
001 Griffiss AFB, NY 13441

306 Cdr, Air Force Avionics Lab
ATTN: AFAL/RWF (Mr. J. Pecqueux)
002 Wright-Patterson AFB, OH 45433

307 AFGL/SULL
S-29
001 HAFB, MA 01731

312 HQ, AFEWC
ATTN: EST
002 San Antonio, TX 78243

314 HQ, Air Force Systems Command
ATTN: DLCA
001 Andrews AFB, Washington, DC 20331

403 Cdr, MIRCOM
Redstone Scientific Info Center
ATTN: Chief, Document Center
002 Redstone Arsenal, AL 35809

404 Crd, MIRCOM
ATTN: DRSMI-RE (Mr. Pittman)
001 Redstone Arsenal, AL 35809

405 Commander
US Army Aereomedical Research Lab
ATTN: Library
001 Fort Rucker, AL 36362

406 Commandant
US Army Aviation Center
ATTN: ATZQ-D-MA
001 Fort Rucker, AL 36362

407 Dir, Ballistic Missile Defense
Advanced Technology Center
ATTN: ATC-R, PO Box 1500
001 Huntsville, AL 35807

418 Commander
HQ, Fort Huachuca
ATTN: Technical Reference Div
001 Fort Huachuca, AZ 85613

419 Commander
US Army Electronic Proving Grnd
ATTN: STEEP-MT
001 Fort Huachuca, AZ 85613

422 Commander
US Army Yuma Proving Ground
ATTN: STEYP-MTD (Tech Library)
001 Yuma, AZ 85364

433 Commander
US Army STC FIO
ATTN: Mr. Robert Miller
001 APO San Francisco, CA 96328

437 Deputy for Science & Technology
Office, Asst Sec Army (R&D)
002 Washington, DC 20310

438 HQDA (DAMA-ARZ-D/Dr. F.D. Verderame)
001 Washington, DC 20310

455 Commandant
US Army Signal School
ATTN: ATSH-CD-MS-E
001 Fort Gordon, GA 30905

456 Commandant
US Army Infantry School
ATTN: ATSH-CD-MS-E
001 Fort Benning, GA 31905

470 Director of Combat Developments
US Army Armor Center
ATTN: ATZK-CD-MS
002 Fort Knox, KY 40121

474 Commander
USA Test & Evaluation Command
ATTN: DRSTE-CT-C
001 Aberdeen Proving Grnd, MD 21005

475 Cdr, Harry Diamond Laboratories
ATTN: Library
2800 Powder Mill Road
001 Adelphi, MD 20783

476 CB Detect & Alarms Div
Chemical Systems Lab
ATTN: DRDAR-CLC-CR (H. Tennenbaum)
002 Aberdeen Proving Grnd, MD 21010

477 Dir, USA Ballistic Research Lab
ATTN: DRXBD-LB
001 Aberdeen Prov Grnd, MD 21005

481 Harry Diamond Laboratories
ATTN: DELHD-R-NM (Dr. J. Nemarich)
2800 Powder Mill Road
001 Adelphi, MD 20783

482 Director
US Material Sys Anal Actv
ATTN: DRXSY-T
001 Aberdeen Prov Grnd, MD 21005

483 Director
US Material Sys Anal Actv
ATTN: DRXSY-MP
001 Aberdeen Prov Grnd, MD 21005

498 Cdr, TARADCOM
ATTN: DRDTA-UL, Tech Library
001 Warren, MI 48090

499 Cdr, TARCOM
ATTN: DRDTA-RH
001 Warren, MI 48090

503 Dir, USA Engineering
Waterways Exper Station
ATTN: Research Ctr Library
002 Vicksburg, MS 39108

507 Cdr, AVRADCOM
ATTN: DRSAV-E
PO Box 209
001 St. Louis, MO 63166

511 Cdr, ARRADCOM
ATTN: DRDAR-LOA-PD
002 Dover, NJ 07801

512 Cdr, ARRADCOM
ATTN: DRDAR-LCN-S (Bldg 95)
001 Dover, NJ 07801

513 Cdr, ARRADCOM
ATTN: DRDAR-TSS, #59
001 Dover, NJ 07801

515 PM, FIREFINDER/REMBASS
ATTN: DRCPM-FER
002 Fort Monmouth, NJ 07703

517 TRI-TAC Office
ATTN: TT-SE
001 Fort Monmouth, NJ 07703

518 Cdr, USA Satellite Comm Agcy
ATTN: DRCPM-SC-3
002 Fort Monmouth, NJ 07703

519 Cdr, USA Avionics Lab
AVRADCOM
ATTN: DAVAA-D
001 Fort Monmouth, NJ 07703

521 Cdr, Project Manager, SOTAS
ATTN: DRCPM-STA
001 Fort Monmouth, NJ 07703

528 Cdr, USA Research Office
ATTN: Dr. David Squire
PO Box 12211
001 Research Triangle Park, NC 27709

529 Cdr, USA Research Office
ATTN: Dr. Horst Wittmann
PO Box 12211
001 Research Triangle Park, NC 27709

531 Cdr, USA Research Office
ATTN: DRXRO-IP
PO Box 12211
002 Research Triangle Park, NC 27709

532 Cdr, US Army Research Office
ATTN: DRXRC-PH (Dr. R.J. Lontz)
PO Box 12211
002 Research Triangle Park, NC 27709

533 Commandant
USA Inst for Military Assistance
ATTN: ATSU-CTD-MO
002 Fort Bragg, NC 28307

537 Cdr, USA Tropic Test Center
ATTN: STETC-Tech-Info Ctr
001 APO Miami 34004

542 Commandant
USAFAS
ATTN: ATSF-CD-DE
001 Fort Sill, OK 73503

554 Commandant
USA Air Defense School
ATTN: ATSA-CD-MS-C
001 Fort Bliss, TX 79916

556 HQ, TCATA
Technical Information Center
ATTN: Mrs. Ruth Reynolds
001 Fort Hood, TX 76544

559 Commander
USA Dugway Proving Ground
ATTN: MT-T-I
001 Dugway, UT 84022

563 Commander, DARCOM
ATTN: DRCDE
5001 Eisenhower Avenue
001 Alexandria, VA 22333

564 Cdr, USA Signals Warfare Lab
ATTN: DELSW-OS
Vint Hill Farms Station
001 Warrenton, VA 22186

567 Commandant
US Army Engineer School
ATTN: ATZA-TDL
002 Fort Belvoir, VA 22060

568 Commander
USA Mobility Eqp Res & Dev Cmd
ATTN: DRDME-R
001 Fort Belvoir, VA 22060

569 Commander
USA Engineer Topographic Labs
ATTN: ETL-TD-EA
001 Fort Belvoir, VA 22060

571 Dir, Applied Tech Lab
USA Rsch & Tech Labs (AVRADCOM)
ATTN: Technical Library
001 Fort Eustis, VA 23604

575 Commander, TRADOC
ATTN: ATDOC-TA
001 Fort Monroe, VA 23561

576 Commander
USA Training & Doctrine Cmd
ATTN: ATCD-IE
001 Fort Monroe, VA 23651

579 PM, Control & Analysis Ctrs
Vint Hill Farms Station
001 Warrenton, VA 22186

602 Cdr, NV&EOL, ERADCOM
ATTN: DELNV-D
001 Fort Belvoir, VA 22060

603 Cdr, Atmospheric Sciences Lab
ERADCOM
ATTN: DELAS-SY-S
001 White Sands Missile Rng, NM 88002

604 Chief, Office of Missile
Electronic Warfare
Electronic Warfare Lab ERADCOM
001 White Sands Missile Rng, NM 88002

606 Chief
Intel Material Dev & Sup Ofc
Electronic Warfare Lab ERADCOM
001 Fort Meade, MD 20755

607 Cdr, Harry Diamond Labs
ATTN: DELHD-CO,TD (In Turn)
2800 Powder Mill Road
001 Adelphi, MD 20783

608 Cdr, ARRADCOM
ATTN: DRDAR-TSB-S
001 Aberdeen Proving Grnd, MD 21005

609 Cdr, ERADCOM
ATTN: DRDEL-CG,CD,CS (In Turn)
2800 Powder Mill Road
001 Adelphi, MD 20783

612 Cdr, ERADCOM
ATTN: DRDEL-CT
2800 Powder Mill Road
002 Adelphi, MD 20783

615 Cdr, ERADCOM
ATTN: DRDEL-SB
2800 Powder Mill Road
001 Adelphi, MD 20783

616 Cdr, ERADCOM
ATTN: DRDEL-SB
2800 Powder Mill Road
001 Adelphi, MD 20783

619 Cdr, ERADCOM
ATTN: DRDEL-PA
2800 Powder Mill Road
Adelphi, MD 20783

620 Cdr, ERADCOM
ATTN: DRDEL-I-TL
2800 Powder Mill Road
Adelphi, MD 20783

680 Commander
US Army Electronics R&D Command
000 Fort Monmouth, NJ 07703

1 DRDEL-SA
1 DELEW-D
1 DELCS-D
1 DELET-DD
1 DELET-DX
1 DELSD-D
1 DELSD-L (Library)
2 DELSD-L-S (Stinfo)
25 Originating Office

681 Commander
US Army Comm R&D Command
000 Fort Monmouth, NJ 07703

1 DRDCO-COM-RO
1 USMC-LNO
1 ATFE-LO-EC

682 Commander
US Army Comm & Electronics
Material Readiness Command
000 Fort Monmouth, NJ 07703

1 DRSEL-PL-ST
1 DRSEL-MA-MP
1 DRSEL-PA

701 MIT Lincoln Laboratory
ATTN: Library (Rm A-082)
002 Lexington, MA 02173

703 NASA Scientific & Tech Info Facility
Baltimore/Washington Intl Airport
001 PO Box 8757, MD 21240

704 National Bureau of Standards
Bldg 225, Rm A-331
ATTN: Mr. Leedy
001 Washington, DC 20231

705 Advisory Group on Electron Devices
201 Varick Street, 9th Floor
002 New York, NY 10014

707 TACTEC
Batelle Memorial Institute
505 King Avenue
001 Columbus, OH 43201

709 Plastics Tech Eval Center
Picatinny Arsenal, Bldg 176
ATTN: Mr. A. M. Anzalone
001 Dover, NJ 07801